J Therm Anal Calorim (2012) 107:541–547
DOI 10.1007/s10973-011-1590-x

Thermal characteristics of bitumen pyrolysis

Hou-yin Zhao · Yan Cao · Song P. Sit · Quentin Lineberry · Wei-ping Pan

Received: 1 February 2011 / Accepted: 14 April 2011 / Published online: 1 May 2011

Abstract The pyrolysis behavior of bitumen was investigated using a thermogravimetric analyzer–mass spectrometer system (TG–MS) and a differential scanning calorimeter (DSC) as well as a pyrolysis-gas chromatograph/mass spectrometer system (Py-GC/MS). TG results showed that there were three stages of weight loss during pyrolysis—less than 110, 110–380, and 380–600 °C. Using distributed activation energy model, the average activation energy of the thermal decomposition of bitumen was calculated at 79 kJ mol^{-1}. The evolved gas from the pyrolysis showed that organic species, such as alkane and alkene fragments had a peak maximum temperature of 130 and 480 °C, respectively. Benzene, toluene, and styrene released at 100 and 420 °C. Most of the inorganic compounds, such as H_2, H_2S, COS, and SO_2, released at about 380 °C while the CO_2 had the maximum temperature peaks at 400 and 540 °C, respectively. FTIR spectra were taken of the residues of the different stages, and the results showed that the C–H bond intensity decreased dramatically at 380 °C. Py-GC/MS confirmed the composition of the evolved gas. The DSC revealed the endothermic nature of the bitumen pyrolysis.

Keywords Bitumen · TG–MS · DAEM · Py-GCMS · DSC

H. Zhao · Y. Cao · Q. Lineberry · W. Pan (✉)
Institute for Combustion Science & Environmental Technology, Western Kentucky University, Bowling Green, KY 42101, USA
e-mail: wei-ping.pan@wku.edu

S. P. Sit
Oil Sands Operations, Cenovus Energy Inc, 421 7th Ave SW, Calgary, AB T2P0M5, Canada

Introduction

With an ever decreasing amount of conventional light oil and increasing global demand for energy and environmental concerns, such as global warming, research into alternative sources of liquid and solid hydrocarbons has increased. Bitumen extracted from oil sands is getting more and more attention [1, 2]. It is a semi-solid material which is mainly obtained from surface mining and thermal in situ extraction of oil sands. Currently, it is either upgraded to synthetic sweet crude before marketed to conventional refineries, or sold directly to coking refineries equipped with cokers and hydrotreaters, where either the sweet synthetic crude or bitumen is refined into transportation fuels. Research has shown that bitumen is a more environmentally friendly and less toxic fuel than coal [3]. Relatively, bitumen produces less particulate, toxic metal and CO_2 emission when combusted. Since pyrolysis is the first step of bitumen conversion processes, such as combustion, hydrotreatment, carbonization, and gasification, it is important to know the characteristics of bitumen pyrolysis at high temperature. Many researchers have studied the characteristics of bitumen at high temperature [4–6]. Schlepp et al. [4] observed that when the temperature was above 300 °C, the bitumen generated light hydrocarbons and an insoluble residue regardless of the presence of water. Benbouzid and Hafsi [5] used the differential method to study the kinetic parameters of pure and oxidized bitumens. Phillips et al. [6] studied the kinetic parameters of the bitumen pyrolysis at 360, 400 and 420 °C, respectively. Bitumen is a heterogeneous material, so it is more suitable to consider the heterogeneous reactions when trying to understand bitumen pyrolysis. Distributed activation energy model (DAEM) is a simplified model for determining kinetic parameters for complex

reactions, which assumes a set of irreversible first-order reactions that have different activation energies, and it does not require a prior assumption or a mathematical model fitting to obtain the kinetic parameters [7–10]. It has been widely used to analyze such complex reactions as pyrolysis of fossil fuels [7], biomass [8–10], and dried sewage sludge [11]. However, it has not been applied to the study of bitumen pyrolysis. The coupling of TG with a Fourier transform infrared (FTIR) spectrometer and/or a mass spectrometer (MS) has been used for the study of coal pyrolysis and biomass pyrolysis [11, 12], but a literature survey shows no application of evolved gas analysis to assist in the understanding of the bitumen pyrolysis mechanism. So in this study, proper kinetic parameters, which can predict the devolatilization behavior of bitumen pyrolysis, were obtained using DAEM. Also, the production of gaseous species during the pyrolysis was examined using thermogravimetric analyzer–mass spectrometer system (TG–MS) and pyrolysis-gas chromatograph/mass spectrometer system (Py-GC/MS). A better understanding of the pyrolysis behavior of bitumen will be beneficial to bench-scale experiments and industrial applications.

Experimental

Materials

Cenovus Energy Inc. provided dry bitumen for this study, which was extracted from Alberta surface mineable oil sands. The proximate and ultimate analysis of the bitumen as received is shown in Table 1. It can be seen that the bitumen is mainly composed of carbon and hydrogen with an atomic ratio of H/C = 1.5, which is less than the H/C ratio of conventional oil of 2.

Table 1 Proximate analysis and ultimate analysis for bitumen

Component	Content/wt%
Proximate analysis	
Moisture	3.1
Volatiles	85.1
Ash	0.1
Heat value/btu lb^{-1}	17792
Ultimate analysis	
C	82.2
H	10.1
O	2.9
N	0.5
S	4.2

FTIR technique

The sample was analyzed by a Perkin Elmer Spectrum One FTIR with a universal attenuated total reflectance attachment. The IR detection range was 650–4000 cm^{-1}.

TG and TG–MS technique

The thermal analysis was carried on a TA 2950 TG analyzer. About 20 mg of the sample was heated from 30 to 600 °C at a rate of 20, 30, 50, or 80 °C min^{-1}, respectively. The experiments took place under a nitrogen atmosphere (purity > 99.999%) with a flow rate of 100 mL min^{-1}.

The TG–MS system consisted of Dupont 951 TG analyzer and a Fisons instruments Thermolab mass spectrometer interfaced via a heated capillary transfer line. The capillary transfer line was heated to 200 °C and the inlet port on the mass spectrometer was heated to 150 °C. The Fisons unit is based on a quadrupole design and the scanned mass range was from 1 to 200 m/z. It uses an electron impact ionization energy of 70 eV. The system is operated at a pressure of 1×10^{-5} torr. 10 mg of the sample was heated from 30 to 600 °C at a rate of 20 °C min^{-1}. The experiments took place under a nitrogen atmosphere (purity > 99.999%) with a flow rate of 50 mL min^{-1}.

DSC technique

Differential scanning calorimeter (DSC) was performed with a TA 2920 DSC analyzer. About 3–6 mg of the sample was placed in an aluminum pan with a pinhole lid and was heated to 600 °C at a rate of 10 °C min^{-1} under a nitrogen flow (purity > 99.999%) of 40 mL min^{-1}.

Py-GC/MS technique

The Py-GC/MS experiments were performed using a CDS 5200 pyrolyzer and a Varian 2200 GC/MS instrument in a helium atmosphere. For the Py-GC/MS experiments, three temperature ranges were examined, which corresponded to the stages seen in the TG experiments. The first stage was from 30 to 110 °C, the second stage was from 110 to 380 °C, and the third stage was from 380 to 600 °C. During the trapping portions of the experiment, the Tenax TA was held at about 40 °C. At the end of each stage, the Tenax TA trap was desorbed at 300 °C and the GC chromatogram was obtained.

In the GC/MS system, helium was the carrier gas and the capillary column used was DB-5: 30 m × 0.25 mm × 0.25 μm. The split ratio was 1:20. The temperature of the transfer line was 300 °C. The temperature program was

as follows: initial temperature of 35 °C for 5 min, ramped to 300 °C at 8 °C min^{-1}, holding for 10 min.

Results and discussion

TG and DSC results

The weight loss data show that there are three stages of thermal decomposition during heating of the sample (Fig. 1). The first stage is from 30 to 110 °C with a weight loss of 1.8%, which may be due to evaporation of water and other small molecular weight compounds. The second stage is from 110 to 380 °C with a weight loss of 43.7% and the third stage is from 380 to 600 °C with a weight loss of 44.3%. Actually the sample continues to decompose after 600 °C, but the weight loss is very small.

The heating rate is one of the most important parameters influencing the thermal decomposition of bitumen. Figure 2 shows that with increasing heating rate, the maximum decomposition rate and the temperature corresponding to the peak decomposition rate increased. When the heating rate increased from 20 to 80 °C min^{-1}, the maximum decomposition rate increased from 10.6 to 36.2% min^{-1} as did the corresponding peak temperature from 476 to 522 °C. This is because with increasing heating rates, the time to reach a given temperature becomes shorter. As a result, more time has to elapse before the reaction is complete, which causes the entire curve to shift to higher temperatures.

From the DSC curve (Fig. 3), we can clearly see endothermic transitions at 290 and 445 °C with the enthalpy of 14 and 83 J g^{-1}, respectively, which are due to the pyrolysis of bitumen.

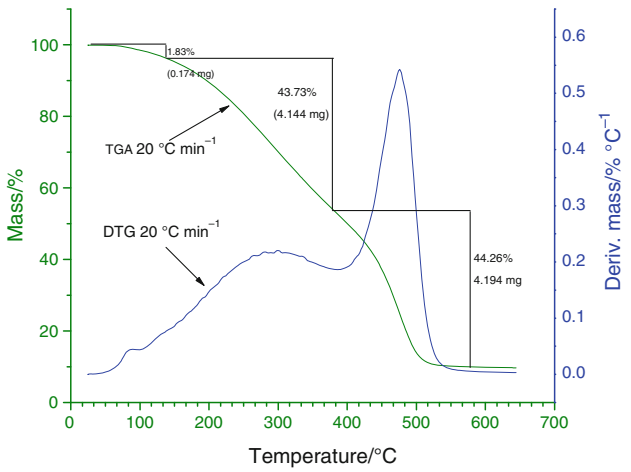

Fig. 1 TGA/DTG curve of bitumen versus temperature under nitrogen flow

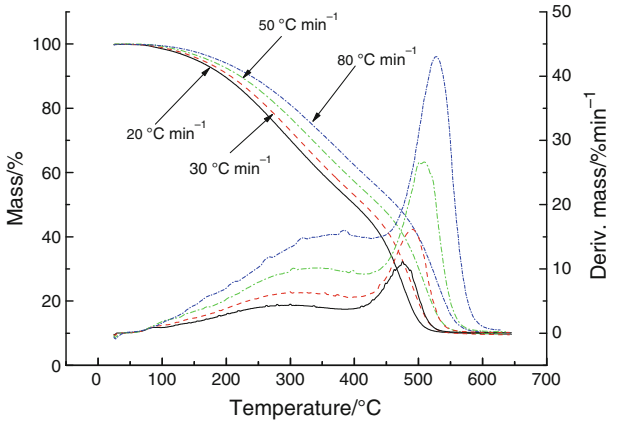

Fig. 2 TGA curve for bitumen versus temperature under nitrogen flow

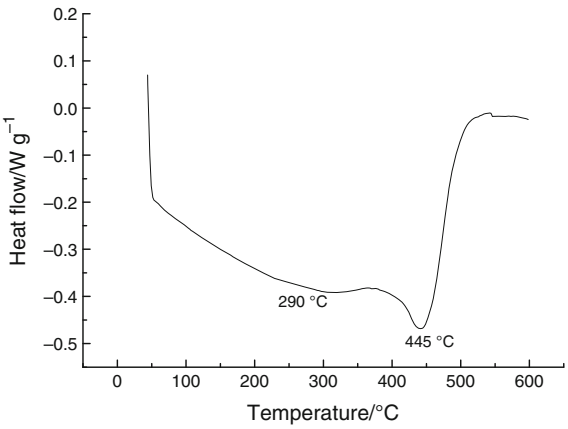

Fig. 3 DSC curve for bitumen versus temperature under nitrogen flow

TG–MS analysis of gas products and FTIR analysis of residue

TG–MS is a very useful technique for studying thermal degradation mechanisms. From TG–MS results, the mass evolution of species with respect to time and temperature can be obtained and these peaks can be matched with the weight loss stages. The mass peaks for bitumen pyrolysis are given in Fig. 4. The major products for the thermal decomposition of bitumen include alkene fragments (*m*/*z* 41, 55, 69, and 83), alkane fragments (*m*/*z* 43, 57, 71, and 85), aromatic compounds (*m*/*z* 78, 91, and 105), and inorganic compounds such as H_2 (*m*/*z* 2), H_2O (*m*/*z* 18), H_2S (*m*/*z* 34), CO_2 (*m*/*z* 44), SO_2 (*m*/*z* 64), and COS (*m*/*z* 60). The evolution of hydrogen began at 420 °C and reached a maximum at 520 °C (Fig. 4b). Water evolution can be identified using *m*/*z* 18, 17, and 16 with a certain ratio (10:6:4) due to the fragmentation pattern. However, the major methane (CH_4) peak also occurs at *m*/*z* 16 with a

fragment of CO_2 also contributing depending on its concentration. Thus, the identification of methane will be based on the additional intensity of the peak at *m*/*z* 16, or a differing peak maximum temperature between *m*/*z* 16 and 18. Water evolving during the first thermal decomposition stage below 150 °C may be due to moisture present in the sample (Fig. 4a). Water continued to release until its peak maximum at 480 °C, which may come from cross linking of hydrocarbons. Hydrogen sulfide was released at 380 °C with a maximum temperature peak at 420 °C (Fig. 4b). Carbonyl sulfide evolved at 380 °C and the release of SO_2 started at 400 °C with a peak maximum temperature at 480 °C (Fig. 4b), which may be due to the thermal decomposition of organic sulfur in the bitumen. Carbon dioxide was observed between 300 and 600 °C and had the maximum temperature peak at 400 and 540 °C, respectively (Fig. 4c). Benzene, toluene, and styrene released at 100 and 420 °C (Fig. 4d). Alkane fragments and alkene fragments had a peak maximum temperature of 130 and 480 °C, respectively (Fig. 4e, f). There is a little delay between DTG curve and evolved gas curve, which is due to the time it takes for the evolved gas to reach the detector.

Based on the total area (arbitrary unit), CO_2, H_2O, alkane, and alkene compounds are the major products of the evolved gas, while SO_2, H_2S, and COS accounts for approximately one-hundredth of the main composition. So the removal of SO_2, H_2S, and COS is an important issue for utilization of bitumen.

The original bitumen and the residue at the end of each stage were analyzed by FTIR (Fig. 5). Table 2 shows that the bitumen is mainly composed of aromatic hydrocarbons, alkanes, and alkenes and a small amount of nitro and sulfide compounds, which is consistent with other researcher [13]. The overall intensity of the FTIR signal at 110 °C decreased slightly compared to the unreacted bitumen. The intensity of the spectrum decreased dramatically as the temperature increased to 380 °C, especially the C–H stretching of alkanes (2921–2853 cm^{-1}) and C–H bending of alkanes (1455 cm^{-1}). By 600 °C, the spectrum was essentially featureless.

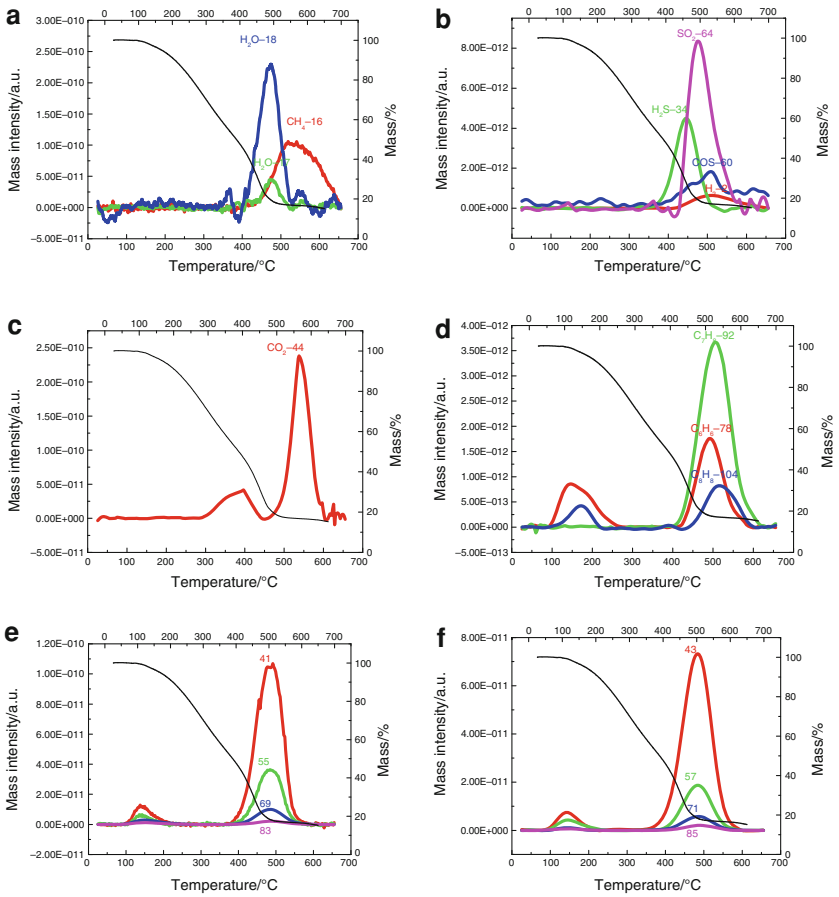

Fig. 4 Mass spectra for bitumen pyrolysis at the heating rate of 20 °C min^{-1} in nitrogen flow (**a** *m*/*z* 16, 17, and 18; **b** *m*/*z* 2, 34, 60, and 64; **c** *m*/*z* 44; **d** *m*/*z* 78, 91, and 105; **e** *m*/*z* 41, 55, 69, and 83; **f** *m*/*z* 43, 57, 71, and 85)

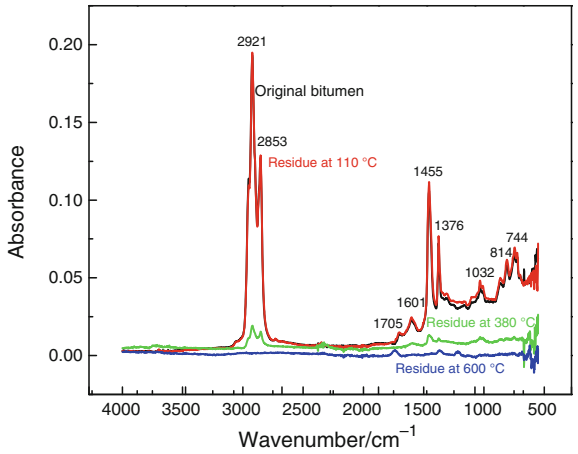

Fig. 5 Overlay of FTIR spectra for original bitumen and residue at 110, 380, and 600 °C

Kinetics analysis

In this study, DAEM was used to obtain the proper kinetic parameters to predict the thermal decomposition of bitumen pyrolysis. According to this method, at least three sets of experimental data obtained under different heating rates are required. When the model is used to analyze bitumen pyrolysis, the DAEM is expressed as [9]:

$$1 - V/V^* = \int_0^\infty \exp\left(-k_0 \int_0^t \mathrm{e}^{-E/RT}\mathrm{d}t\right) f(E)\mathrm{d}E \quad (1)$$

where V is the volatile against time t, V^* is the total volatile in the bitumen, $f(E)$ is the distribution function of activation energy E, and k_0 is the pre-exponent factor corresponding to E value. The function $f(E)$ satisfies

$$\int_0^\infty f(E)\mathrm{d}E = 1 \quad (2)$$

Equation 1 was simplified to Eq. 3 by Miura [14, 15]:

$$V/V^* = 1 - \int_{Es}^\infty f(E)\mathrm{d}E = \int_0^{Es} f(E)\mathrm{d}E \quad (3)$$

In the simplified model, the Arrhenius equation can be described as follows:

$$\ln\left(\frac{a}{T^2}\right) = \ln\left(\frac{k_0 R}{E}\right) + 0.6075 - \frac{E}{RT} \quad (4)$$

where $a = \mathrm{d}T/\mathrm{d}t$, the heating rate of pyrolysis. By using Eq. 4, Arrhenius plots can be drawn for $\ln(a/T^2)$ versus 1/T at the selected V/V^* values for different a values. If two heating rates are used, a series of E values can be calculated from the slopes of the straight lines at different V/V^* levels. In this study, four heating rates (a = 20, 30, 50, and 80 °C min^{-1}) were chosen to reduce error. The Arrhenius plot of a/T^2 versus $1/T$ that was used to obtain the activation energy, E, at selected level of V/V^* is given in Fig. 6. From the linear slope and intercept of the plot, the activation energy, E, and pre-exponent factor, k_0, can be obtained. Figure 7 shows the relationship between activation energy, E, and bitumen conversion, V/V^*. It can be seen that with increasing temperature and conversion, E increases. In the first stage, the conversion is about 1.8%, and the average activation energy is 57 kJ mol^{-1}. While the conversion increases to 20%, the average activation energy remains constant at 57 kJ mol^{-1}. This is because, in the beginning, the breaking of the weakest links in the chain, for example heteroatom chemical bonds and active group as well as the evaporation of small molecular weight compounds are in priority. As the conversion increases to 50% in the second stage, the activation energy increases to 70 kJ mol^{-1}, which may be due to the cracking of the side chain chemical bonds. When the conversion is more than 50%, the activation energy dramatically increases from 75 to 115 kJ mol^{-1}. This is because at this stage, the backbone chains are broken.

Table 2 FTIR results for bitumen

Wave number	Attribution of the FTIR main absorption bands
2921, 2853	H–C–H asymmetric and symmetric stretch of alkanes
1705, 1601	C=C stretching of alkenes
1455	C–H bending of alkanes
1376	N–O stretching of nitro groups
1306	C=S stretching
<1300	C–C stretching of alkanes

The k_0 value corresponding to E can be calculated by using Eq. 4. The relationship between k_0 and E are shown in Fig. 8. It can be seen that the k_0 value increased from an order of 10 to an order of 10^4 s^{-1}, while the E increased from 50 to 115 kJ mol^{-1}. With increasing of E, the k_0

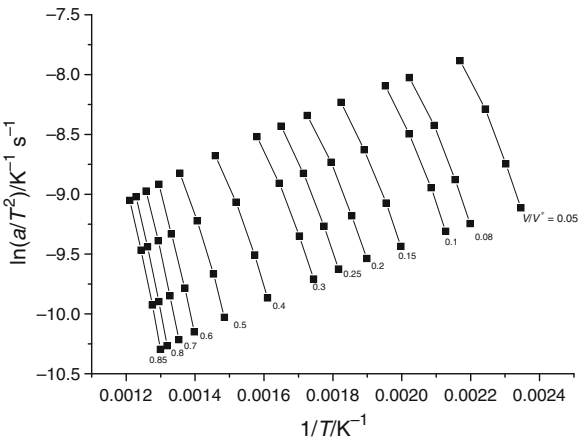

Fig. 6 Arrhenius plot of $\ln(a/T^2)$ versus $1/T$ at selected V/V^* value for the bitumen

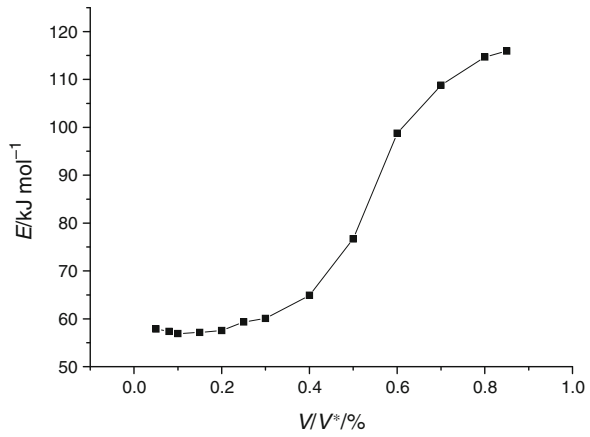

Fig. 7 Relationship between activation energy E and conversion V/V^*

exponentially increased, which would compensate for the decrease of reaction rate constant caused by increasing activation energy. This relationship is compensation effect [16].

Pyrolysis-GC/MS analysis

Figure 9 shows an overlay of the total ion chromatograms for the different stages of the Py-GC/MS experiment. It can be seen that the composition shifted from low molecular weight compounds (C6–C10) and mid molecular weight compounds (C11–C15) to high molecular weight compounds (>C15) when the temperature increased from 110 to 380 °C, while at 600 °C, not only were low and mid molecular weight compounds still present, but also high molecular weight compounds were evolved.

In the first stage (less than 110 °C), highly volatile compounds (high vapor pressure or low boiling point compounds) and mid molecular weight compounds (C10–C15) were evolved. In this stage, low molecular weight

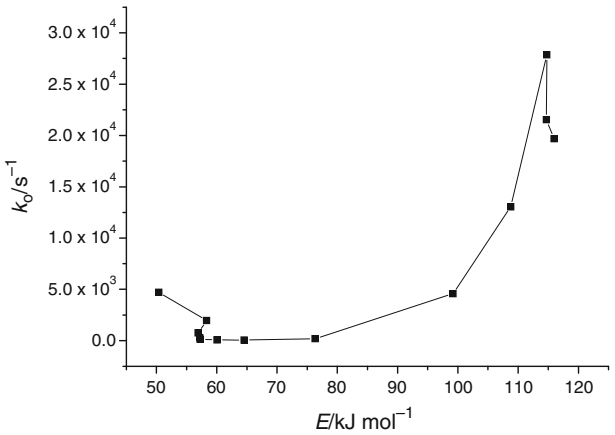

Fig. 8 Relationship between pre-exponential factor k_0 and activation energy E

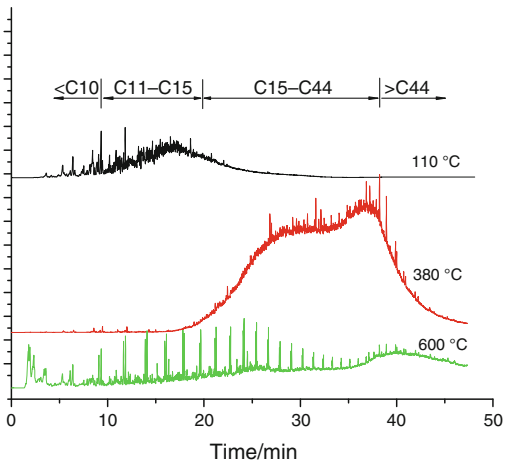

Fig. 9 Overlay of total ion chromatogram for bitumen at different temperatures

compounds such as 4-dimethyl-hexane and 3-ethyl-hexane evaporated and small fragments resulting from the cleavage of heteroatom bonds evolved, so the average activation energy at this stage is small (57 kJ mol^{-1}), which is less than that of the second and the third stages. Also in this stage, the existence of thiophene compounds indicates the presence of organic sulfur in the sample.

According to the mechanism of thermal degradation of polymeric materials, after the side-group elimination in the first stage, the decomposition is mainly composed of random scission [17], so in the second stage (110–380 °C), with increasing temperature, small fragments of varying chain lengths are produced as the side chains are cleaved from the main chain. As a result, high molecular weight compounds (>C15) predominated over low and mid molecular weight compounds.

In the third stage (380–600 °C), the pyrolysis was very complex. From Fig. 5 we can see that after the second stage, the intensity of all functional groups has decreased dramatically, so in the third stage unimolecular or quasi unimolecular reactions dominate. These processes result in the release of low molecular weight compounds (C6–C10), mid molecular weight compounds (C10–C15), and high molecular weight compounds (>C15). So the average activation energy is the highest in this stage, 109 kJ mol^{-1}. In this stage, a regular series of peaks appears resulting from the release of a series of hydrocarbons (C10–C44),

Table 3 Composition of bitumen pyrolysis at 110, 380, and 600 °C (area of total peaks)

Carbon number	110 °C area/%	380 °C area/%	600 °C area/%
C6–C10	63.5	11.3	27.6
C11–C15	36.5	8.4	26.2
C15–C44	–	80.3	46.2

each one carbon larger than the peak before. The peaks actually appear as doublets–one for the alkane and the other for the alkene form of the hydrocarbon. Table 3 shows that the low and mid molecular weight compounds account for about 53% of the emission while the high molecular weight compounds account for 46%.

Conclusions

The thermal behavior of bitumen pyrolysis has been investigated using TG, Py-GC/MS as well as DSC. The kinetic parameters were determined using DAEM. Also the evolution of gaseous species was monitored with respect to temperature using TG–MS. The following conclusions have been drawn:

- TG results showed that there were three stages of thermal decomposition during heating of the sample—less than 110, 110–380, and 380–600 °C.
- When the $V/V^* < 0.20$, the average activation energy was 57 kJ mol^{-1} and when the $V/V^* > 0.50$, the average action energy was 104 kJ mol^{-1}. The pre-exponent factor changed from 10 to 10^4 s^{-1}.
- The evolved gas is composed of organic compounds such as alkene and alkane fragments and inorganic compounds such as H_2O, CO_2, and SO_2. Most of the organic compounds had a peak maximum temperature of 130 and 480 °C and inorganic compounds released at about 380 °C.
- The Py-GC/MS results showed that the composition of bitumen pyrolysis was mainly composed of n-alkanes, n-alkenes, and oxidized compounds. During the first stage, it was mainly composed of low and mid molecular weight compounds while during the second stage, the comparative amount of compounds larger than C15 was about 80%. In the third stage, low and mid molecular weight compounds comprised about 53% while the high molecular weight compounds accounted for 46%.

Since H_2S, SO_2, and COS evolved during bitumen pyrolysis, the next step is to find useful catalysts to decrease the SO_X content and improve the CO_2 concentration.

Acknowledgements We gratefully acknowledge financial supports through projects by Cenovus, Canada.

References

1. Pakdel H, Roy C. Recovery of bitumen by vacuum pyrolysis of Alberta tar sands. Energy Fuel. 2003;17:1145–52.
2. Park YC, Paek JY, Bae DH, Shun D. Study of pyrolysis kinetics of Alberta oil sand by thermogravimetric analysis. Korea J Chem Eng. 2009;26:1608–12.
3. Orimulsion and power stations. http://www.parliament.uk/post/pn084.pdf.
4. Schlepp L, Elie M, Landais P, Romero M. Pyrolysis of asphalt in the presence and absence of water. Fuel Process Technol. 2001;74:107–23.
5. Benbouzid M, Hafsi S. Thermal and kinetic analyses of pure and oxidized bitumens. Fuel. 2008;87:1585–90.
6. Phillips C, Haidar N, Poon YC. Kinetic models for the thermal cracking of athabasca bitumen: the effect of the sand matrix. Fuel. 1985;64:678–91.
7. Liu XG, Li BQ, Miura K. Analysis of pyrolysis and gasification reactions of hydrothermally and supercritically upgraded low-rank coal by using a new distributed activation energy model. Fuel Process Technol. 2001;69:1–12.
8. Li CS, Suzuki K. Kinetic analysis of biomass tar pyrolysis using the distributed activated energy model by TG/DTA technique. J Therm Anal Calorim. 2009;98:261–6.
9. Sonobe T, Worasuwannarak N. Kinetic analyses of biomass pyrolysis using the distributed activation energy model. Fuel. 2008;87:414–21.
10. Scott SA, Dennis J, Davidson J, Allan H. Thermogravimetric measurements of the kinetics of pyrolysis of dried sewage sludge. Fuel. 2006;85:1248–53.
11. Shao JG, Yan R, Chen HP, Wang BW, Lee DH. Pyrolysis characteristics and kinetics of sewage sludge by thermogravimetry fourier transform infrared analysis. Energy Fuel. 2008;22:38–45.
12. Dumanli AG, Tas S, Yurum Y. Co-firing of biomass with coals, part 1. Thermogravimetric kinetic analysis of combustion of fir (*Abies bornmulleriana*) wood. J Therm Anal Calorim. 2011;103:925–33.
13. Holleran G, Sc B App, Sc M. App, Compositionally controlled bitumen for quality. http://www.slurry.com/techpapers/techpapers_contrbit.shtml.
14. Miura K. A new and simple method to estimate $f(E)$ and $k_0(E)$ in the distributed activation energy model from three sets of experimental data. Energy Fuel. 1995;9:302–7.
15. Miura K, Maki T. A simple method for estimating $f(E)$ and $k_0(E)$ in the distributed activation energy model. Energy Fuel. 1998;12:846–9.
16. Lakshmanan CC, Bennett ML, White N. Implications of multiplicity in kinetic parameters to petroleum exploration: distributed activation energy models. Energy Fuel. 1991;5:110–7.
17. Pielichowski KR, Pielichowski K, Njuguna J. Thermal degradation of polymeric materials. Shrewsbury: Smithers Rapra Technology; 2005. p. 30.